Journal of Atomic and Molecular Sciences

ISSN 2075-1303

Global Science Press

Nonlinear optical properties of metal/metal free porphyrins and their graphene oxide composites in picosecond regime

Received Nov.1, 2017,
Accepted Dec. 17, 2017,

DOI: 10.4208/jams.110117.121717a

http://www.global-sci.org/jams/

Jiancai Leng[a], Jie Sun[a] and Yujin Zhang[a],*

Abstract. The nonlinear optical properties of porphyrins (Cu porphyrin, Zn porphyrin and H_2MHTP) and their covalently linked composites with graphene oxide (GO) have been studied by numerically solving the rate equations and field intensity equation with an iterative predictor-corrector finite-difference time-domain technique. The three-level scheme is introduced to illustrate the interaction between the molecules and laser in picosecond time domain. The optical limiting and dynamical two-photon absorption are investigated. Our numerical results show that GO-porphyrin composites show enhanced nonlinear absorption properties compared with individual porphyrin molecules due to the strong electron acceptor capability of the GO moeity, which agrees with the experimental measurements. Moreover, the dependence of the thickness of the absorber and the pulse duration on the two-photon absorption cross sections of the medium are discussed, indicating that one can modulate the dynamical two-photon absorption process by regulating the paremeters of the medium and the laser.

1. Introduction

As a newly appeared material, graphene has exhibited remarkable nonlinear optical (NLO) properties, which makes it attracting enormous scientific attention for the potential applications in photonic and optoelectronic fields such as in data storage, optical limmiting (OL) etc. [1-4]. Traced back to the most beginning, Wang et al. firstly reported the broadband NLO and OL properties of graphene dispersions with nanosecond pulses at wavelength of 532 and 1064 nm [5]. Their measurments show that nonlinear scattering (NLS), originating from the thermally induced solvent bubbles and microplasmas, are responsible for this nonlinear response. In addition, Liu et al. studied the NLO properties of graphene oxide (GO) with good solubility in nanosecond and picosecond regimes at 532 nm [6], showing that two-photon absorption (TPA) dominated the nonlinear absorption in picosecond regime, while excited state absorption (ESA) plays an important role in nanosecond regime. To further modify the NLO properties of graphene, the covalent or non-covalent functionalization of GO with fullerenes [7], porphyrin [8], oligothiophene [9,10], Fe_3O_4 nanoparticles [11], and phthalocyanine [12] have been synthesized and studied. These functionalized GO hybrid materials exhibit good NLO behaviors with high NLO absorption coefficients in nanosecond and femtosecond timescale regimes due to the successful formation of donor-acceptor system and the combination of different NLO mechanisms.

It has been shown that porphyrins have many potential applications in optoelectronics, nonlinear optics [13]. Furthermore, metal substituted porphyrins have shown better third order NLO properties than metal free porphyrins [14-16]. Recently, a serious of novel covalent GO with different metal or mental free porphyrins were synthesized experimentally and their NLO properties were explored in picosecond regime [17,18]. However, there is rare theoretical study on the optical properties of graphene or its porphyrin composite. This phenomenon mainly attribute to two reasons: firstly, the limitation of the computational capacity makes theoretical calculation for these complicated systems on the ab-initio level really difficult; secondly, NLO properties of graphene oxide-porphyrin composite depend strongly on the dynamical parameters of the interaction between laser field and the medium.

In this paper, we present a dynamical theory of the sequential TPA for laser pulses and theoretically study the enhanced NLO and OL properties in metal or metal free porphyrins (Cu porphyrin, Zn porphyrin and H_2MHTP) and their covalently functionalized GO-porphyrin composites (GO-Cu porphyrin, GO-Zn porphyrin and GO-H_2MHTP) with an iterative predictor-corrector finite-difference time-domain (FDTD) technique by numerically solving the rate equation-field intensity equation. Our numerical results show that all the compounds exhibit outstanding OL performance, which will be useful for sensors or human eye protection and stabilization of light sources for optical communications. In addition, GO-porphyrin composites show enhanced nonlinear absorption properties compared with individual porphyrin molecules, and GO-metal porphyrins show more obvious nonlinear absorption properties compared with GO-metal free porphyrins in picosecond time scales.

2. Theoretical methods

As is referred to Ref. [19,20], we have reduced the studied compounds to a simplified model of three-level system: the ground state S_0 the first excited state S_1 and the higher excited state S_2 due to the good overlap and energy transfer between the energy levels of the porphyrins and the GO. This scheme

[a] School of Science, Qilu University of Technology (Shandong Academy of Sciences), Jinan 250353, China

has taken into account two sequential TPA channels S_0 to S_1 and S_1 to S_2, as shown in Figure 2.1(b).

2.1. Rate equations for a three-level system

The populations of S0, S1, S2 states for a three-level system obey the generalized rate equations:

$$\begin{aligned}
\frac{\partial}{\partial t}\rho_{S_0} &= -\gamma_{S_0S_1}(\rho_{S_0}-\rho_{S_1}) - \gamma_{S_0S_2}(\rho_{S_0}-\rho_{S_2}) + \Gamma_{S_1}\rho_{S_1}, \\
\frac{\partial}{\partial t}\rho_{S_1} &= \gamma_{S_0S_1}(\rho_{S_0}-\rho_{S_1}) - \gamma_{S_1S_2}(\rho_{S_1}-\rho_{S_2}) - \Gamma_{S_1}\rho_{S_1} + \Gamma_{S_2}\rho_{S_2}, \\
\frac{\partial}{\partial t}\rho_{S_2} &= \gamma_{S_0S_2}(\rho_{S_0}-\rho_{S_2}) + \gamma_{S_1S_2}(\rho_{S_1}-\rho_{S_2}) - \Gamma_{S_2}\rho_{S_2},
\end{aligned} \tag{1}$$

Where Γ_{S0}, Γ_{S1}, Γ_{S2}, are the decay rates of the states S_0, S_1, S_2 respectively. The total populations are normalized to one:

$$\sum_{n=0}^{2}\rho_{S_n} = 1. \tag{2}$$

It is convenient to express one-photon induced transitions (form S0 to S1 and form S1 to Sn) rates γ_{S0S1} andγ_{S1S2} through the transition dipole moments d_{S0S1}, d_{S1S2} or the corresponding one-photon absorption (OPA) cross section σ_{S0S1}, σ_{S1S2}, , under rotating wave approximation (RWA).

$$\begin{aligned}
\gamma_{S_0S_1}(t) &= \frac{\left|\boldsymbol{d}_{S_0S_1}\right|^2 I(t)}{\hbar^2 c\varepsilon_0}\frac{\Gamma}{\Omega_{S_0S_1}^2+\Gamma^2} = \frac{\sigma_{S_0S_1}I(t)}{\hbar\omega}\frac{\Gamma^2}{\Omega_{S_0S_1}^2+\Gamma^2}, \\
\gamma_{S_1S_2}(t) &= \frac{\left|\boldsymbol{d}_{S_1S_2}\right|^2 I(t)}{\hbar^2 c\varepsilon_0}\frac{\Gamma}{\Omega_{S_1S_2}^2+\Gamma^2} = \frac{\sigma_{S_1S_2}I(t)}{\hbar\omega}\frac{\Gamma^2}{\Omega_{S_1S_2}^2+\Gamma^2}, \\
\Omega_{S_0S_1} &= \omega-\omega_{S_0S_1},\ \Omega_{S_1S_2} = \omega-\omega_{S_1S_2},
\end{aligned} \tag{3}$$

Where ω is the input light frequency, I(t) is the instantaneous intensity of the field, and Γ is the homogeneous broadening of the spectral line. We assume $\hbar\Gamma_{mn} = \hbar\Gamma = 0.1eV$ for all transitions. Ω_{S0S1} and Ω_{S1S2} are the detuning of light frequency from resonant frequency.

Similarly, the rate γ_{SOS2} of two-photon induced transition from S0 to S2 is defined through the TPA cross section σ_{SOS2} as follows:

$$\gamma_{S_0S_2} = \frac{\sigma_{S_0S_2}I^2(t)}{2\hbar\omega}\frac{\Gamma^2}{(2\omega-\omega_{S_0S_2})^2+\Gamma^2}, \tag{4}$$

2.2. Field intensity equation

In the case of the picosecond pulse propagating along the z axis through thin media, where the role of self-focusing and defocusing is small, the change of **the** refraction and the transverse of the field can thus be neglected. The absorption of the field can be described by field intensity equation:

$$\left(\frac{\partial}{\partial z}+\frac{1}{c}\frac{\partial}{\partial t}\right)I(t) = -N[\sigma^{(1)}I(t)+\sigma^{(2)}I^2(t)]. \tag{5}$$

For our studied system, the total OPA cross section $\sigma^{(1)}$ and TPA cross section$\sigma^{(2)}$ are expressed as:

$$\sigma^{(1)} = \sigma_{S_0S_1}(\rho_{S_0}-\rho_{S_1}) + \sigma_{S_1S_2}(\rho_{S_1}-\rho_{S_2}),\ \sigma^{(2)} = \sigma_{S_0S_2}(\rho_{S_0}-\rho_{S_2}). \tag{6}$$

2.3. Calculation of the dynamical TPA cross section

When regardless of significant recombination, diffuse and thermal runaway, the differential equation of the field intensity can be expressed as [21],

$$dI/dz + \alpha I + \beta I^2 = 0, \tag{7}$$

Where α denotes the linear absorption coefficient and β is the TPA coefficient. The analytical solution can be reformed as follows:

$$1/T(z) = I_0/I(z) = \exp(\alpha z) + \left[\exp(\alpha z)-1\right]\beta I_0/\alpha, \tag{8}$$

here T(z) is the transmission of the field intensity at the propagation distance z.

As to a strong input electric field, the TPA coefficient dependents strongly on the input intensity I_0 [22]:

$$\beta = \beta_0 - \xi I_0, \tag{9}$$

Where β_0 is the steady-state TPA coefficient and ε is a constant. Plug equation (9) into (8), one can notice the inverse transmission 1/T(z) is a quadratic function of the input field intensity I_0,

$$\frac{1}{T(z)} = \frac{I_0}{I(z)} = \exp(\alpha z) + \frac{\left[\exp(\alpha z)-1\right]\beta_0}{\alpha}I_0 - \frac{\left[\exp(\alpha z)-1\right]\xi}{\alpha}I_0^2. \tag{10}$$

By fitting equation (10) properly, the absorption coefficients α and β_0 can be determined. The relationships between molecular TPA cross section σ_{tp} and β_0 can thus be expressed as below:

$$h\nu\beta_0 = \sigma_{tp}N, \tag{11}$$

where $h\upsilon$ is the incident photon energy, N is the molecular density.

2.4. Computational details

Here we investigate the OL behaviors of three different porphyrins (Zn porphyrin, Cu porphyrin, H_2MHTP) and covalently functionalized GO- (Zn porphyrin, Cu porphyrin, H2MHTP) composites. Their structures are shown in Figure 2.1(a). To perform numerical simulations, the resonant transition energies, OPA cross sections, and relaxation rates, TPA coefficient of these compounds are extracted from the experiments [8,17,23]. The corresponding values are collected in Table 2-1. Unfortunately, the TPA cross section σ_{S0S2} is not available in the literatures. Thus we determined the values of σ_{S0S2} through the relationship in equation (11). In order to save the computation time, the simulations are performed for relatively high concentration and short distance compared with experimental conditions. Fortunately, the numerical results can be compared with the measurements according to the scaling relation $N_{theo}L_{theo}=N_{exp}L_{exp}$ where L_{theo}=0.48 mm, L_{exp}=1.0 cm. Using the above scaling relation, we get the simulation concentrations N_{theo} as $6.33\times10^{23}/m^3$ and $4.84\times10^{23}/m^3$ for porphyrins and composites, respectively.

As for the input electric field, we choose a hyperbolic secant shape incident pulse

$$E(z,t=0) = F_0\,\mathrm{sech}\left[1.76(z/c+z_0/c)/\tau_p\right]\cos\left[\omega(z+z_0)/c\right] \tag{12}$$

with the peak amplitude F_0 which has a relationship with field intensity of $I(t)=\frac{c\varepsilon_0|F_0(t)|^2}{2}$. where τp is the full width at half maximum (FWHM) of the pulse intensity profile, ω is the carrier wave frequency of the incident pulse $\omega=2\pi c/\lambda$. In order to match the experimental results, the laser parameters are set to τ_p =30 ps, λ=352 nm, The choice of Z_0 ensures that the pulse penetrates negligibly into the medium when t=0.

Table 2-1: Photophysical parameters of porphyrins and their GO composites [17], including the resonant transition energy E, OPA cross section σ, the relaxation rate of the singlet state Γ, and the TPA coefficient β.

Samples	E_{S0S1} (eV)	E_{S1S2} (eV)	σ_{S0S1} 10^{-23} m^2	σ_{S1S2} 10^{-23} m^2	FOM ($\sigma_{S0S1}/\sigma_{S1S2}$)	Γ_{S1} 10^9 S^{-1}	Γ_{S2} 10^9 S^{-1}	β 10^{-10} cm/W
H_2MHTP	2.3995	0.5542	2.1	2.2	10.2	9.2	2.8	0.17
GO-H_2MHTP	2.5353	0.5147	5.5	15.0	27.3	6.4	0.65	36.2
Cu Porphyrin	2.2805	0.6940	4.2	7.2	17.2	0.9	6	0.21
GO-Cu Porphyrin	2.2763	0.6565	8.4	24.7	29.4	0.5	7	120.4
Zn Porphyrin	2.2035	0.6883	4.6	9.6	21.0	0.78	5	2.5
GO-Zn Porphyrin	2.2000	0.6788	5.2	20.2	38.8	1.41	9	134.2

3. Results and discussion

To study the physical mechanism of OL effect, Zn porphyrin and GO-Zn porphyrin are selected as the samples to characterize the pulse propagation process. To better match the experimental analysis, the duration of the incident pulse is set as 30ps and the corresponding peak intensity is equal to $I_0=2\times10^{10}$ W/cm^2. Figure 3.1(a) demonstrates the temporal evolution of the pulse intensity envelope at different propagation distances. As shown in Figure 3.1(a), due to the interaction between the field and medium, energies are transformed from the field to the medium, thus one can clearly observe that the pulse intensities decrease rapidly during propagation. Furthermore, the decrease extent in GO-Zn porphyrin is relatively much greater, which indicates that GO-Zn porphyrin possesses better OL behavior.

In picosecond pulse regime, the incoherent two-step TPA can dominate the coherent one-step TPA process and the populations excited to S2 state decay rapidly back to S1 state due to its rather short lifetime (ps) [24]. So particles are mainly excited from the ground state S0 to the OPA state S1, while the TPA state S2 is populated slightly. Figure 3.1(b) displays the temporal evolution of population differences between level S0 and S1 at different propagation distances. Due to their excellent TPA characteristics, when z=0.012 mm, there are approximately 30 percent of the particles excited to level S1, while the change extent in Zn porphyrin is much gradual. It is apparent that the change range of population differences in Zn porphyrin and GO-Zn porphyrin becomes small during pulse propagation. This may attribute to that during the interaction between the medium and field, particles are being absorbed, and the pulse intensity decreases during pulse propagation.

Figure 3.2 shows the intensity dependent NLO transmission of porphyrins and GO-porphyrin composites. The light transmittance is the ratio of transmission intensity to incident intensity. When the incident intensity is relatively weak, the medium show constant transmittance, indicating linear absorption process. While increasing the incident intensity, the transmittance decreasing remarkably. Furthermore, the decrease extent in GO-porphyrin composites even more sharply than in single porphyrins, which indicates the former possess better OL ability. Figure 3.3(b) reveals the transmittance as a function of the thickness of the medium for porphyrins and composites. It is obvious that for a certain compound, the transmittance decreases as the propagation distance increases. The main mechanism is that interaction between field and medium would be enhanced with the propagation distance increased, thus more energy transfers from field to medium during the pulse propagation. Consistent with Figure 3.1(a), Figure 3.1(b) reveals that composites show preferable OL behaviors than single porphyrin molecules due to the larger ratio of excited state absorption cross section and ground state absorption cross section (FOM).

The OL curves are plotted and shown in Figure 3.3 for Cu-porphyrin, Zn-porphyrin, H_2MHTP and GO-porphyrin composite materials in ps time scales. The OL behaviors of the compounds are clearly demonstrated as expected. From our theoretical results, GO composite materials show enhanced limiting abilities compared with individual porphyrins, for GO-porphyrin composite helps in achieving stronger nonlinear absorption, TPA and NLS leading to better OL materials. Mental porphyrins with GO show enhanced nonlinear absorption behaviors compared to mental free porphyrin with GO for porphyrin with heavier central metal has better OL performance due to the faster intersystem crossing caused by the enhanced spin-orbit coupling [15]. Namely, the OL abilities of these materials increase in this order: GO-Zn porphyrin> GO-Cu porphyrin> GO H_2MHTP> Zn porphyrin> Cu porphyrin> H_2MHTP. The tendency corresponds well with the experimental FOM values as shown in Table2-1.

By numerical fitting the output and input intensity relation in the OL region at the propagation distance of 0.48mm, one can get the TPA coefficient β_0 of GO-Zn porphyrin, GO-Cu porphyrin, GO H_2MHTP, Zn porphyrin, Cu porphyrin, H_2MHTP as 0.9746×10^{-11} m/W, 0.8479×10^{-11} m/W, 0.2830×10^{-11} m/W, 0.1930×10^{-11} m/W, 0.1652×10^{-11} m/W, 0.1332×10^{-11} m/W respectively. The results match quite well with the experimental in trend but somewhat smaller or larger. The discrepancy between our numerical results and the measurements may result from the off-measurement condition in measurement.

Through the relationships between molecular TPA cross section σ_{tp} and β_0 in equation (11), the dynamical TPA cross section are obtained as 7.5192×10^4 GM, 6.5424×10^4 GM, 2.1836×10^4 GM, 1.1583×10^4 GM, 0.9743×10^4GM, 0.7857×10^4 GM for GO-Zn porphyrin, GO-Cu porphyrin, GO-H_2MHTP, Zn porphyrin, Cu porphyrin, H_2MHTP respectively(1GM=1×10^{-50}

cm^4s/photon). These values are relatively larger than that of other organic molecules. From the results we can find that introducing the GO into porphyrin can effectively enhance the nonlinear absorption ability of compound due to its special highly conjugated two-dimensional structure and rich delocalized π-electron.

To elucidate the effect of pulse duration on the TPA cross section, we give out the TPA coefficient β_0 and the corresponding TPA cross section σ_{tp} for these six compounds with different pulse width at the propagation distance of 0.48mm (Table 3-1). It is obvious that for these compounds the TPA cross section strongly and positively depends on the pulse width, which can be attributed to that longer pulse increases the probability of the transition from the intermediate state S1 to the TPA state S2 and enhances the sequential two-step TPA cross section.

Table 3-1: The values of TPA coefficient β_0(10^{-11} m/W) and TPA cross section σ_{tp} (10^4 GM) 1GM=1×$10^{-50}$$cm^4s$/photon with different input pulse width at the same propagation distance of 0.48 mm, N=N_{theo}.

τ	9 ps		30 ps		100 ps	
Samples	β_0	σ_{tp}	β_0	σ_{tp}	β_0	σ_{tp}
H2MHTP	0.1312	0.7739	0.1337	0.7889	0.1349	0.7956
Cu Porphyrin	0.1631	0.9624	0.1693	0.9988	0.1799	1.0617
Zn Porphyrin	0.1929	1.1380	0.1975	1.1649	0.2019	1.1914
GO-H2MHTP	0.2805	2.1643	0.2900	2.2376	0.3038	2.3439
GO-Cu Porphyrin	0.9228	7.1202	0.9514	7.3407	0.9879	7.6221
GO-Zn Porphyrin	1.0220	7.8852	1.0418	8.0378	1.0331	8.1409

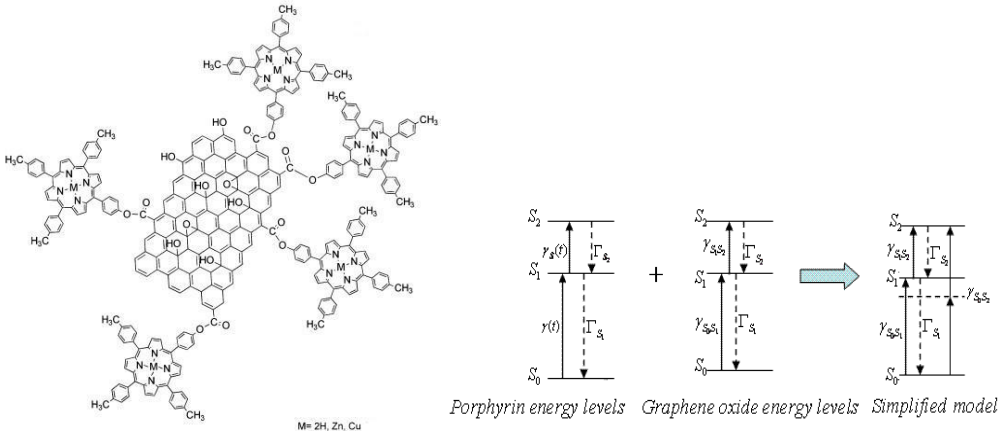

(a) (b)

Figure 2.1. (a) The structures of composites and (b) schematic energy-level diagram of GO-porphyrin composites and their simplified model.

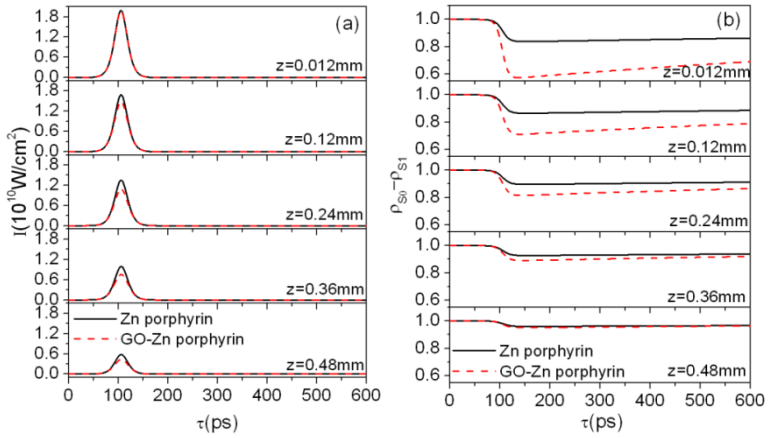

Figure 3.1: (a) The temporal evolution of the pulse intensity envelope and (b) population differences between the states S0 and S1 at different propagation distances of 0.012mm,0.12mm,0.24mm,0.36mm,0.48mm,(τ=30 ps, I_0=2×10^{10} W/cm^2, N=Nt_{heo}).

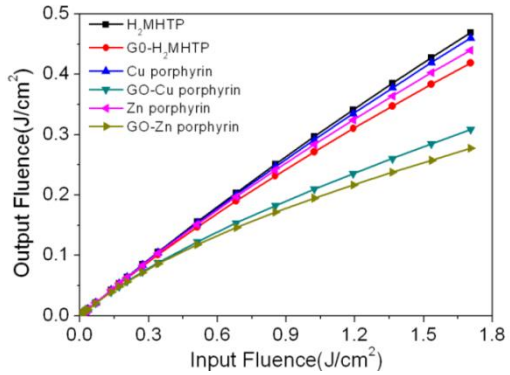

Figure 3.2: Output fluence versus input fluence for different compounds (Z=0.48 mm, τ =30 ps, N=N_{theo}).

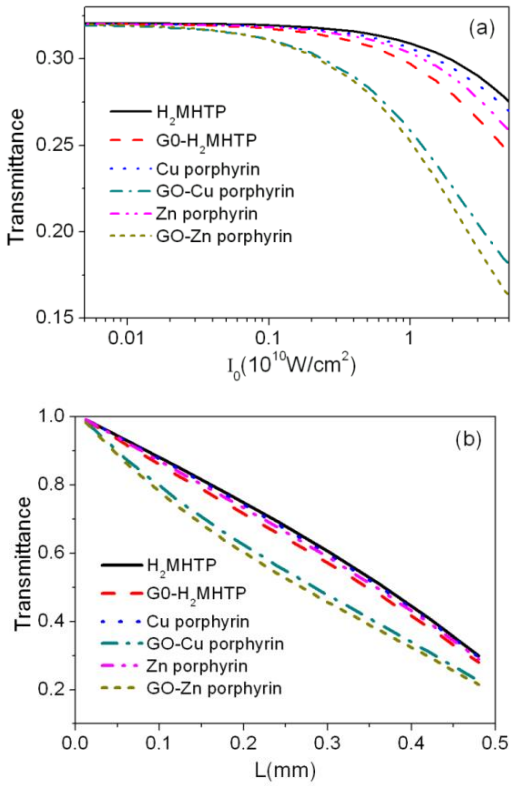

Figure 3.3: Transmittance as a function of (a) the intensity of the incident field through the absorbing medium (Z=0.48 mm, τ=30 ps, N=Ntheo) and (b) the thickness of the medium for porphyrins and composites (τ=30 ps, I_0=2×10^{10} W/cm^2, N=N_{theo})

4. Conclusions

A simple three-level scheme is introduced to illustrate the TPA mechanism of GO with different metal porphyrins and metal free porphyrins. The NLO properties of the compounds are illustrated by numerically solving coupled rate equations and field intensity equation based on RWA and slowly varying envelope approximation (SVEA) using an iterative predictor-corrector FDTD method in picosecond time scale. Our numerical results show that all this composite materials show significant nonlinear absorption properties due to the strong electron acceptor capability of the GO molecule. Transmittance is a decrease function of the input laser intensity and the propagation distance. GO-porphyrin composites show enhanced nonlinear absorption compared with individual porphyrin molecules, which is consistent with the experimental measurement that larger FOM value leads to more preferable OL and TPA abilities. Besides, the dynamical TPA cross sections are got by fitting output and input intensity relation curves, the results indicates that the pulse duration plays key role on the TPA cross section of the medium.

Acknowledgements

This work was supported by the National Natural Science Foundation of China Grant No. 11704209.

References

[1] Q. Bao and K. P. Loh, *ACS Nano* **6** (2012) 3677.
[2] F. Bonaccorso, Z. Sun, T. Hasan and A. C. Ferrari *Nat. Photonics* **4** (2010)611.
[3] Z. Sun, T. Hasan, F. Torrisi, D. Popa, G. Privitera, F. Q. Wang, F. Bonaccorso, D. M. Basko and A. C. Ferrari, *ACS Nano* **4** (2010) 803.
[4] C. G. Lee, X. D. Wei, J. W. Kysar and J. Hone *Science* **321** (2008)385.
[5] J. Wang, Y. Hernandez, M. Lotya, J. N. Coleman and W. J. Blau *Adv. Mater.* **21**(2009) 2430.
[6] Z. B. Liu, Y. Wang, X. L. Zhang, Y. F. Xu, Y. S. Chen and J. G. Tian *Appl. Phys. Lett.* **94** (2009)021902.
[7] X. Y. Zhang, Z. B. Liu, Y. Huang, X. J. Wan, J. G. Tian, Y. F. Ma and Y. S. Chen *J. Nanosci. Nanotechnol.* **9**(2009) 5752.
[8] J. C. Leng, L. Y. Zhao, Y. J. Zhang and H. Ma J. Phys. Soc. Jpn. **85** (2016) 094401.
[9] Y. S. Liu, J. Y. Zhou, X. L. Zhang, Z. B. Liu, X. J. Wan, J. G. Tian, T. Wang and Y. S. Chen *Carbon* **47** (2009) 3113.
[10] X. L. Zhang, X. Zhao, Z. B. Liu, Y. S. Liu, Y. S. Chen and J. G. Tian *Opt. Express* **17** (2009) 23959.
[11] X. L. Zhang, X. Zhao, Z. B. Liu, S. Shi, W. Y. Zhou, J. G. Tian, Y. F. Xu and Y. S. Chen *J. Opt.* **13** (2011) 075202.
[12] X. Zhao, X. Q. Yan, Q. Ma, J. Yao, X. L. Zhang, Z. B. Liu and J. G. Tian *Chem. Phys. Lett.* **577** (2013) 62.
[13] M. O. Senge, M. Fazekas, E. G. A. Notaras, W. J. Blau, M. Zawadzka, O. B. Locos and E. M. N. Mhuircheartaigh *Adv. Mater.* **19** (2007) 2737.
[14] P. P. Kiran, D. R. Reddy, A. K. Dharmadhikari, B. G. Maiya, G. R. Kumar and D. N. Rao *Chem. Phys. Lett.* **418** (2006) 442.
[15] M. Calvete, G. Y. Yang and M. Hanack *Synth. Met.* **141**(2004) 231.
[16] E. G. A. Notaras, M. Fazekas, J. J. Doyle, W. J. Blau and M. O. Senge *Chem. Commun.* (2007) 2166.
[17] M. B. M. Krishna, N. Venkatramaiah and D. N. Rao *J. Opt.* **16** (2014) 015205.
[18] M. B. M. Krishna, N. Venkatramaiah, R. Venkatesan, D. N. Rao, P. Predeep, M. Thakur and M. K. R. Varma *Optics: Phenomena, Materials, Devices, and Characterization* **1391** (2011) 680.
[19] H. Ma, J. Leng, M. Liu, L. Zhao and Y. Jiao Opt. Commun. **350** (2015) 144.
[20] H. Ma, J. Leng, M. Liu, L. Zhao and Y. Jiao J. Nonlinear Optic. Phys. Mat. **24** (2015) 1550046.
[21] J. D. Bhawalkar, G. S. He and P. N. Prasad *Rep. Prog. Phys.* **59** (1996)1041.
[22] G. S. He, Q. D. Zheng, A. Baev and P. N.Prasad *J. Appl. Phys.* **101** (2007)083108.
[23] M. B. M. Krishna, V. P. Kumar, N. Venkatramaiah, R. Venkatesan and D. N. Rao *Appl. Phys. Lett.* **98** (2011) 081106.
[24] C. K. Wang, P. Zhao, Q. Miao, Y. P. Sun and Y. Zhou *J. Phys. B: At. Mol. Opt. Phys.* **43** (2010)105601.